Hierarchical structure and phase transition of $(GeTe)_n(Sb_2Te_3)_m$ used for phase-change memory

Jino Im,[1] Jae-Hyeon Eom,[1,*] Changwon Park,[1] Kimin Park,[1] Dong-Seok Suh,[2] Kijoon Kim,[2] Youn-Seon Kang,[2] Cheolkyu Kim,[2] Tae-Yon Lee,[2] Yoonho Khang,[2] Young-Gui Yoon,[3] and Jisoon Ihm[1,†]

[1]*Department of Physics and Astronomy, Center for Theoretical Physics, Seoul National University, Seoul 151-747, Korea*

[2]*Materials Center, Samsung Advanced Institute of Technology, Mt. 14-1, Nongseo-Ri, Giheung-Eup, Yongin-Si, Gyeonggi-Do, 449-712, Korea*

[3]*Department of Physics, Chung-Ang University, Seoul, Korea*

(Received 28 July 2008; published 21 November 2008)

$(GeTe)_n(Sb_2Te_3)_m$ is the material which has been extensively studied for phase-change memory applications. However, the local structure and the phase-transition mechanism of this material are not precisely known yet. We propose here, based on the recent extended x-ray absorption fine structure spectroscopy, stibnite-like Sb_2Te_3 units and chainlike GeTe units as primary building blocks of the material. Then we further propose a three-dimensional model of secondary building blocks composed of a small number of primary building blocks. The phase change between the crystalline and the amorphous structure is shown to occur via reorientations of the secondary building blocks, establishing a simple reversible transformation process that can explain the high endurance and the fast switching time of the material. In the amorphous phase, the relaxed structure obtained from the *ab initio* total-energy minimization calculations satisfies the experimentally observed $8-N$ rule for the atomic coordination number.

DOI: 10.1103/PhysRevB.78.205205 PACS number(s): 61.43.Dq, 61.43.Bn, 71.15.Nc

I. INTRODUCTION

Small-size, high-speed, and large-capacity nonvolatile memory (NVM) devices become essential to the development of the multimedia technology in recent years, and the phase-change memory (PCM) is believed to be one of the most promising candidates for the future NVMs.[1,2] The $(GeTe)_n(Sb_2Te_3)_m$ pseudobinary system, usually abbreviated as GST, has been known to satisfy material requirements for the PCM.[3–6] Although GST's are already in use for the rewritable CD and DVD and their commercial application to the random access memory is expected in the near future as well, neither the local structure of the material nor the change in the structure during the phase transition is well established. The high phase-transition speed and the long lifetime, together with the fact that the allowed stoichiometry in the material composition is restricted to $(GeTe)_n(Sb_2Te_3)_m$, strongly suggest that the structure in the amorphous phase may not be truly random. Rather, these materials may conceivably be composed of relatively stable building blocks, and the switching between the crystalline and the amorphous phase can be achieved by a relatively simple rearrangement of the building blocks. Then the questions are: what are the three-dimensional structures of the building blocks and how are they arranged in space with respect to each other? Although several building blocks have been proposed in the literature based on the bond-length information,[7–9] the relation between the crystalline rocksalt phase and the amorphous phase remains poorly understood. Recently, a systematic study on the coordination number (CN) of Ge, Sb, and Te atoms was reported using the extended x-ray absorption fine-structure spectroscopy (EXAFS) experiment.[10] They measured the bond length and the CN for each atomic species for different compositions n and m. They found, among other things, that the total CN satisfies the so-called $8-N$ rule in all composition ranges. In this study, based on these experimental data, we propose a structural model which provides the structural characteristics of the amorphous phase, as well as the mechanism of the phase change between the amorphous and the crystalline structure. This model consists of hierarchical building blocks: primary building blocks are simply stibnite-like Sb_2Te_3 and chainlike GeTe units, and secondary building blocks are composed of larger structural units (consisting of these primary units) which retain structural identities throughout the phase transition. The phase transition can be achieved by local reorientations and relaxations of these secondary building blocks in the present model. Furthermore, first-principles density-functional total-energy minimization calculations presented below show that CN's in the amorphous phase satisfy the $8-N$ rule, in agreement with experimental data.

II. BUILDING BLOCK MODEL

A. Primary building block

In order to explain our structural model, we first introduce the smallest (primary) building blocks. The crystalline $(GeTe)_n(Sb_2Te_3)_m$ obtained during the phase-change device operation is known to have the cubic (rocksalt) structure.[11] In decomposing and analyzing the structure in terms of building blocks, it is natural to consider unit cells of the crystalline GeTe and the crystalline Sb_2Te_3. We examine Sb_2Te_3 first. The crystalline Sb_2Te_3 turns out to have a hexagonal (tetradymite) structure and hence not suitable for the starting point to construct the building block of the GST. It is noted that the chalcogenides Sb_2Se_3 (antimonselite) and Sb_2S_3 (metastibnite) have the stibnite structure whose local structure resembles the cubic structure;[12,13] the stibnite unit cell consists of four subunits whose shape fits to the simple-cubic lattice. Figure 1 shows the unit cell of the stibnite structure and its subunit comprising five strongly bonded atoms,

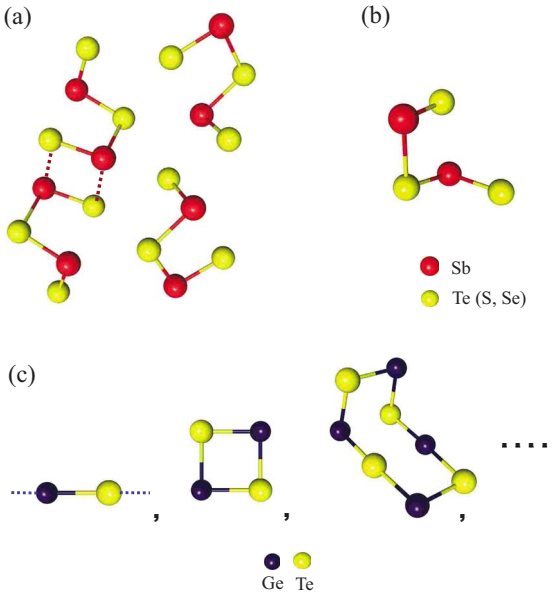

FIG. 1. (Color online) Building blocks of Sb_2Te_3 and GeTe. (a) Unit cell of the stibnite structure. Yellow (light gray) dots indicate S, Se, or Te atoms and the red (gray) ones Sb atoms. (b) A subunit of the stibnite structure in (a), which is our proposed building block of Sb_2Te_3. (c) Proposed structural building blocks of GeTe. Blue (dark gray) dots are Ge atoms and yellow (light gray) ones Te atoms.

which may be regarded as a part of the rocksalt structure. The local structure of the amorphous Sb-Te compound is also observed to be rocksalt like.[14] Thus the stibnite-like Sb_2Te_3 subunit in Fig. 1(b) is a good candidate for the building block of the GST structure, which may exist persistently in both crystalline (rocksalt) and amorphous phases.

On the other hand, since the crystalline GeTe itself has a cubic (rocksalt) structure, the unit cell (Ge-Te) is a natural building block as shown in the first part of Fig. 1(c). However, when we study the phase transition to the amorphous phase later, it is necessary to know how the smallest GeTe units are connected to each other. In other words, we need some structural information on a larger scale because the simple GeTe unit, if it were isolated, would have too many dangling bonds. We note that many chalcogenide compounds (alloys with at least one group VI element S, Se, or Te) like to form a chainlike structure.[15] We propose that the multiple units of GeTe tend to form a chainlike structure in the amorphous phase as exemplified in Fig. 1(c). This chainlike (not necessarily linear) structure is immediately adapted to the rocksalt structure because Ge and Te atoms alternate in the chain as in the rocksalt structure. Later in this section, we will construct the rocksalt structure of the crystalline GST by suitably positioning these two kinds of building blocks.

B. Prediction of the coordination number from the model

Now we study the CN's of the amorphous phase from the above building block model. We first examine some experimental results which are critical to the description of the amorphous structure. It is widely accepted from many experiments that atoms in the amorphous phase satisfy the $8-N$ rule for the CN, namely, the CN of Ge, Sb, and Te are 4, 3, and 2, respectively. Experiments also indicate that there exist almost no Te-Te bonds even if the material becomes amorphous.[10,16] Under these conditions, predictions of our model for the CN are calculated for variable ratios between n and m in $(GeTe)_n(Sb_2Te_3)_m$. The number of Ge, Sb, and Te atoms in $(GeTe)_{1-x}(Sb_2Te_3)_x$ are $1-x$, $2x$, and $1+2x$, respectively, and we investigate the CN as a function of x (for example, $x=\frac{1}{3}$ corresponds to $n=2$ and $m=1$). We start with the $x=0$ case (GeTe). The condition of no Te-Te bonding results in the Ge-Te alternating chain structure because the CN of Te is two and Te has no other choice than having two Ge atoms as nearest neighbors (Ge atoms cannot repeat in this chain as the number of Ge and Te atoms are identical). Since two extra bonds are necessary for each Ge in order to satisfy Ge atom's CN of 4, the Ge-Ge bonds are newly formed by cross linking (i.e., sticking) of neighboring chains of GeTe. In the other extreme of $x=1$, as mentioned above, each building block is Sb_2Te_3 in the stibnite structure [Fig. 1(b)] and these building blocks should be arranged and connected so as to satisfy the CN of 3 and 2 for Sb and Te, respectively. This constraint means, since the Te-Te bond is not allowed, each of the two Te atoms at the end of the Sb_2Te_3 unit in Fig. 1(b) has one extra bond with a Sb atom in a neighboring Sb_2Te_3 unit. One Te atom in the middle of the Sb_2Te_3 unit already has the CN of 2 and no extra bond is allowed. Each of the two Sb atoms inside the unit should have one extra bond with a Te atom in a neighboring Sb_2Te_3 unit. (We can easily prove that Sb-Sb bonds become possible only for $0<x<1$ due to the constraint originating from the given total number of each atomic species.)

A remaining problem is the bonding between GeTe and Sb_2Te_3 units in the general case of $0<x<1$. Here we make a plausible assumption that each of the two unsaturated Te atoms at the end of the Sb_2Te_3 units has no preference of bonding with a particular atom (Ge or Sb), and the relative probability of being Te's nearest neighbor is proportional to the available number of unsaturated Ge or Sb bonds in the material. (This condition is not strict and may be relaxed without changing the result appreciably.) The same assumption of no favor between Ge and Sb is made for bonding of

TABLE I. The predicted coordination number (CN) for each atom as a function of x in amorphous $(GeTe)_{1-x}(Sb_2Te_3)_x$.

Atom	Neighboring atom	CN
Ge	Ge	$2(1-x)^2$
	Sb	$2x(1-x)$
	Te	$2(1+x)$
Sb	Ge	$(1-x)^2$
	Sb	$x(1-x)$
	Te	$2+x$
Te	Ge	$\frac{2(1-x^2)}{1+2x}$
	Sb	$\frac{2x(2+x)}{1+2x}$
	Te	0

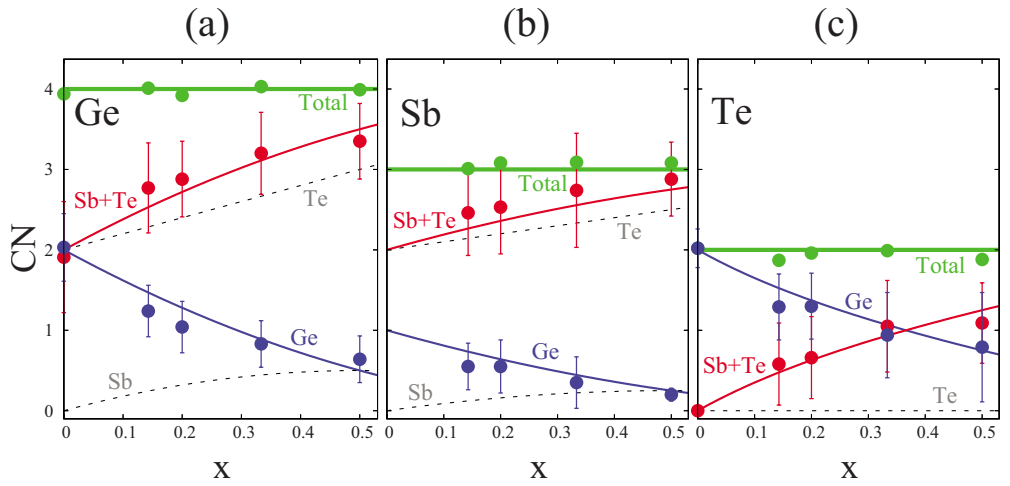

FIG. 2. (Color online) Coordination number (CN) in the GST. CN's of each atom in $(GeTe)_{1-x}(Sb_2Te_3)_x$ are shown in comparison with the EXAFS data. Dots are experimental data (Ref. 10) and curves are calculated results from the formula in Table I. The numbers of nearest-neighbor Sb and Te atoms are calculated (dashed curves), but the sum of the two is indicated in red solid curves (labeled Sb+Te) since the EXAFS cannot distinguish between the two as nearest neighbors.

each Sb atom, which requires one extra bond other than the two nearest-neighbor Te atoms in Sb_2Te_3. Another useful knowledge is that the total number of, for example, Ge-Sb bonds around Ge atoms in the whole material should be identical to that of Sb-Ge bonds around Sb atoms. (In fact, these obvious equalities for the number of heteronuclear bonds dramatically simplify the calculation of CN's.) With the above information, the CN's of Ge, Sb, and Te atoms with different atomic species are completely determined and we summarize the result in Table I. Our predicted results and experimental data of Matsunaga *et al.*[10] for the CN as a function of x for $(GeTe)_{1-x}(Sb_2Te_3)_x$ are compared in Fig. 2. Since Sb and Te atoms cannot be distinguished as a nearest neighbor in the EXAFS, the sum of Sb and Te atoms is also presented in Figs. 2(a)–2(c) and the entire results agree very well with experiment.

C. Secondary building block and relaxation

Although we obtained correct CN's in the amorphous phase, we should also be able to explain how one phase easily evolves into the other (between amorphous and crystalline). One of the simplest ways of introducing disorder at a relatively low-energy cost is the rotation of a certain structural unit. Now we construct a secondary building block by attaching the GeTe unit(s) into the stibnite Sb_2Te_3 unit(s). A secondary building block (or a secondary structural motif) is defined to be a small assembly of primary building blocks which rotates as a whole, while retaining its overall shape, during the phase change. In the case of $Ge_1Sb_2Te_4$, the shape of the secondary building block is chosen to be a cube (with one vacancy site) as shown in Fig. 3(a). This is the smallest secondary block in $Ge_1Sb_2Te_4$ and there could be other kinds of them.[17] (The results for the CN's obtained in Sec. II B are essentially unchanged by introducing the secondary building block.) The secondary building block is not necessarily unique for given n and m. However, the number of different kinds of secondary building blocks must be very small, if not one, because their size and shape should be adequate for an easy rotation inside the bulk material. Vacancies provide additional room and freedom for the movement of the structural unit. In the present work, we focus on $Ge_1Sb_2Te_4$ because of its simplicity from the building block point of view. The crystalline structure accommodates eight secondary building blocks of $Ge_1Sb_2Te_4$ in the $4\times4\times4$ cubic atomic sites [Fig. 3(b)]. To mimic the amorphous structure, each secondary building block in the cube is rotated with all three Euler angles ϕ, θ, and ψ (Ref. 18) chosen randomly [Fig.

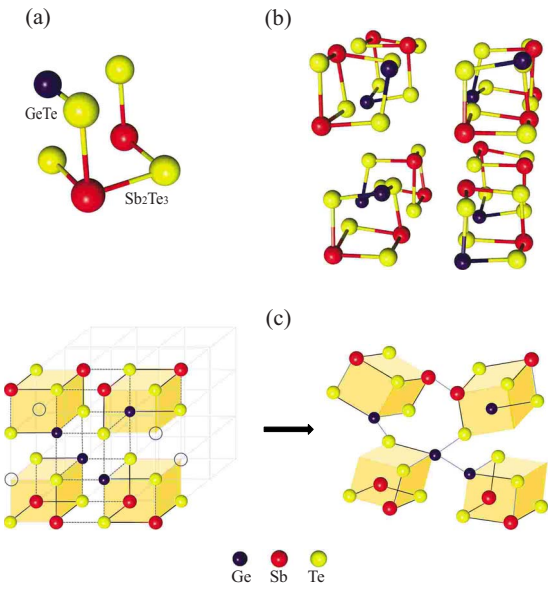

FIG. 3. (Color online) Structure of the $Ge_1Sb_2Te_4$. (a) A secondary building block of $Ge_1Sb_2Te_4$ consisting of one GeTe and one Sb_2Te_3 unit. (b) The supercell used in the simulation which accommodates eight secondary building blocks in (a). (c) An example of rotated secondary building blocks in the cubic supercell. Only four out of eight secondary building blocks are shown for visual clarity. Blue (dark gray), red (gray), and yellow (light gray) dots represent Ge, Sb, and Te atoms, respectively.

3(c)]. Atomic positions are then relaxed allowing for bond breaking and bond formation. The relaxed atomic positions and the equilibrium volume are obtained from the energy minimization. Throughout the energy minimization calculations, we use *ab initio* density-functional pseudopotential methods with the local-density approximation. We employ a plane-wave basis scheme[19] for the expansion of the electronic wave functions with the spin-orbit averaged pseudopotentials of Bachelet *et al.*[20] The local exchange-correlation potential by Gonze *et al.*[21] is used. Brillouin-zone (BZ) averages are performed using the Monkhorst and Pack scheme[22] with $3\times3\times3$ grid points. We use the supercell geometry with 64 atomic sites in the $4\times4\times4$ cubic cell. The plane-wave energy cutoff of 50 Ry is chosen for the self-consistent calculation of the wave functions.

III. RESULTS AND DISCUSSION

Here, we recapitulate our procedure and examine detailed results. We started with building a model structure for a crystalline phase. We assembled secondary building blocks such that the overall configuration looks like a rocksalt structure with vacancies as previously shown in Fig. 3(b). We then relaxed the atomic positions using the energy minimization and obtained the relaxed structure as shown in Fig. 4(a). This is our proposed crystalline structure of $Ge_1Sb_2Te_4$. In order to mimic the amorphous phase, we first randomly rotated secondary building blocks with respect to the unrotated configuration in Fig. 3(b) and obtained a few different configurations as shown in Fig. 3(c) as one of the examples. We then relaxed these rotated structures and Figs. 4(b)–4(d) show three examples of such relaxed structures. Before the random rotation, there exists a distinction between the intrabonding (bonding between atoms inside a single secondary building block) and the interbonding (bonding between atoms belonging to two different secondary building blocks). The intrabond is typically short and the interbond is typically long. On the other hand, we observe in Figs. 4(b)–4(d) that the relaxed geometry after the full rotation shows a lot of short bonds cross linking between different building blocks. The overall atomic configuration looks random, which must be the case since we intend to simulate an amorphous phase in Figs. 4(b)–4(d). The structural relaxation induces a distortion on some secondary building blocks and occasionally a few building blocks are broken. (However, it is interesting to note that, if we examine the structure very closely, most secondary building blocks retain their original shapes more or less.) These cross linking and distortions are natural ways to change the local order in the amorphous phase. It is possible to say that the stibnite structural units of Sb_2Te_3 are connected by the chainlike GeTe in many places. The equilibrium lattice constant is calculated for each configuration. Without rotation, the equilibrium lattice constant of the $4\times4\times4$ cubic cell is 12.0 Å, but the rotation of building blocks induces a volume expansion. The average volume increase in the rotated configurations is about 8%, which is comparable with the experimental value of 7%.[23,24]

In order to check the applicability of our model further, bond lengths and coordination numbers are calculated for the

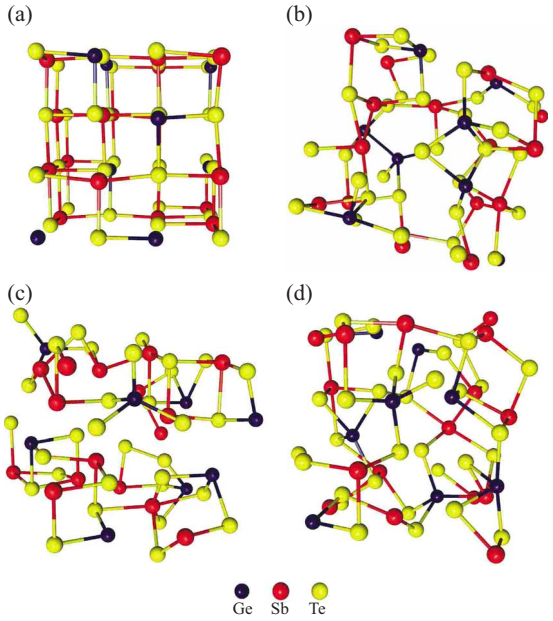

FIG. 4. (Color online) Relaxed structures of the $Ge_1Sb_2Te_4$. (a) The relaxed structure without the rotation of building blocks, simulating the crystalline phase. (b)–(d) The relaxed structure after all building blocks are rotated in different directions, simulating the amorphous phase. Blue (dark gray), red (gray), and yellow (light gray) dots represent Ge, Sb, and Te atoms, respectively.

relaxed configurations. The results are summarized in Table II. In the crystalline phase, calculated bond lengths (shorter ones) are 2.85 and 2.96 Å for Ge-Te and Sb-Te, comparable with the EXAFS values[7] of 2.83 ± 0.01 and 2.91 ± 0.01 Å, respectively, as listed in Table II. The CN's for the crystalline rocksalt phase are nominally 6, 6, and 6-δ (δ=1.5 for $Ge_1Sb_2Te_4$ and 1.2 for $Ge_2Sb_2Te_5$, originating from vacancies) for Ge, Sb, and Te, respectively. However, after relaxation, the separation between shorter and longer bonds occurs and the CN's are reduced significantly if we count the shorter bonds only. In the amorphous phase, we average the CN's of the three rotated building block configurations in Figs. 4(b)–4(d). Although calculated bond lengths (2.74 and 2.90 Å) are somewhat larger than the values from recent EXAFS and further experiment (2.61 ± 0.02 and 2.85 ± 0.02 Å),[16] characteristic changes of the bonds during the phase transition between the crystalline and amorphous phase are well reproduced in our model. Bond lengths decrease compared with the crystalline phase and the calculated CN's almost obey the $8-N$ rule. However, we note that there are small discrepancies in the CN's of Ge and Te, i.e., undercoordinated Ge and overcoordinated Te. In detail, Ge has both threefold and fourfold coordinations in our calculation. These two configurations of Ge produce different structural values in bond lengths and angles. The geometry of the fourfold coordinated Ge shows the typical tetrahedral bonding characters, while the geometry of the threefold coordinated Ge resembles the local structure of the crystalline phase (the angle between a pair of two bonds is 90°). If we count only fourfold Ge cases for the bond length, then the bond length decreases from 2.74 Å (weighted average of both fourfold and threefold cases) down to 2.6 Å. This value is very close

TABLE II. Bond length and coordination number (CN) of $Ge_1Sb_2Te_4$ obtained from energy minimization calculations. The crystalline phase here means the relaxed geometry of the unrotated building block configuration, and the amorphous phase is the relaxed geometry of the fully rotated building block configuration. In the crystalline phase, the CN includes the short bonds only. (The nominal CN's in the rocksalt structure are given in parentheses.) In the amorphous phase, three different configurations in Figs. 4(b)–4(d) are averaged. Since experimental data for the crystalline phase of $Ge_1Sb_2Te_4$ are not available to us, those of $Ge_2Sb_2Te_5$ are presented.

	Bond length (Å)		CN		
	Ge-Te	Sb-Te	Ge	Sb	Te
Crystal.(expt.)	2.83[a]	2.91[a]			
Crystal.(calc.)	2.85	2.96	3.0(6)	3.2(6)	2.4(4.5)
Amorph.(expt.)	2.61[b]	2.85[b]	3.91[b]	3.12[b]	1.98[b]
Amorph.(calc.)	2.74	2.90	3.58	3.17	2.41

[a]Reference 7 (crystalline $Ge_2Sb_2Te_5$).
[b]Reference 16.

to experimental data, which is 2.61 ± 0.02 Å according to Jòvàri *et al.*[16] Regarding the overcoordinated Te, it is not clear why we still have an appreciable number of threefold coordinated Te atoms, and our simulation is yet to be improved to agree better with experiment.

On retrospect, the fairly good agreement of CN's with experiment is anticipated to a certain extent and not too surprising. Once our building block model is assumed, the primary building blocks have the CN of 2 for both Ge and Sb and 4/3 (on the average) for Te as opposed to almost 6 for Ge and Sb, and $6-\delta$ for Te (as explained above) in the crystalline rocksalt structure. The formation of the secondary structure somewhat increases the values of CN's, and the final amorphous structure has even larger CN's by cross linking the blocks so as to achieve the chemically most stable CN's (i.e., $8-N$ rules). The fact that the CN's of our proposed model for the crystalline phase are, if the shorter bonds only are counted, much smaller than the nominal CN's for the rocksalt structure and rather similar to the amorphous phase supports this scenario. We can call the final configuration as the "tertiary structure" in the hierarchy of the structural formation. The crystalline and the amorphous phases differ only in the tertiary structure. According to our model, the recrystallization from the amorphous phase may be achieved easily by rotating randomly oriented building blocks back to the original well-aligned structure of the crystalline phase, without changing the number of short bonds significantly. The existence of this simple reversible process should lead to the high endurance (i.e., long material lifetime) and a fast switching time of the GST.

IV. CONCLUSIONS

In this study, we propose a structural model for the amorphous $(GeTe)_n(Sb_2Te_3)_m$ based on three-dimensional building blocks. We employ hierarchical building blocks: a GeTe chain and a stibnite Sb_2Te_3 are chosen as primary building blocks and their composites as secondary building blocks. In our model, the phase change between the amorphous and the crystalline structure is explained by the reorientation of the secondary building blocks and their relaxation. Calculated equilibrium volumes and bond lengths using *ab initio* computational methods are comparable with experimental data, and the CN's of the amorphous phase are shown to satisfy the $8-N$ rule.

ACKNOWLEDGMENTS

This work is supported by the KOSEF grant funded by the Korea Government MEST (Center for Nanotubes and Nanostructured Composites), the Korea Research Foundation under Grant No. KRF-2005-070-C00041, and the Korea Government MOEHRD under Basic Research Fund No. KRF-2006-341-C000015. The authors also acknowledge the computational support from KISTI under the 6th Strategic Supercomputing Applications Support Program.

*Present address: ICES, University of Texas at Austin, Austin, TX 78712, USA.
†jihm@snu.ac.kr

[1] H. Goronkin and Yang Yang, MRS Bull. **29**, 805 (2004).
[2] M. H. R. Lankhorst, B. W. Ketelaars, and R. A. Wolters, Nature Mater. **4**, 347 (2005).
[3] A. Pirovano, A. L. Lacaita, A. Benvenuti, F. Pellizzer, and Roberto Bez, IEEE Trans. Electron Devices **51**, 452 (2004).
[4] I. Friedrich, V. Weidenhof, W. Njoroge, P. Franz, and M. Wuttig, J. Appl. Phys. **87**, 4130 (2000).
[5] J. González-Hernández, E. Prokhorov, and Yu. Vorobiev, J. Vac. Sci. Technol. A **18**, 1694 (2000).

[6] H. F. Hamann, M. O'Boyle, Y. C. Martin, M. Rooks, and H. K. Wickramasinghe, Nature Mater. **5**, 383 (2006).
[7] A. V. Kolobov, P. Fons, A. I. Frenkel, A. N. Ankudinov, J. Tominaga, and T. Uruga, Nature Mater. **3**, 703 (2004).
[8] D. A. Baker, M. A. Paesler, G. Lucovsky, S. C. Agarwal, and P. C. Taylor, Phys. Rev. Lett. **96**, 255501 (2006).
[9] Z. Sun, J. Zhou, and R. Ahuja, Phys. Rev. Lett. **98**, 055505 (2007).
[10] T. Matsunaga, N. Yamada, and M. Sato (http://support.spring8.or.jp/TU/040325_9.pdf).
[11] S. Shamoto, N. Yamada, T. Matsunaga, Th. Proffen, J. W. Richardson, Jr., J.-H. Chung, and T. Egami, Appl. Phys. Lett. **86**, 081904 (2005).
[12] P. Arun and A. G. Vedeshwar, J. Mater. Sci. **31**, 6507 (1996).
[13] A. P. Torane and C. H. Bhosale, J. Phys. Chem. Solids **63**, 1849 (2002).
[14] K. Tani, N. Yiwata, M. Harigaya, S. Emura, and Y. Nakata, J. Synchrotron Radiat. **8**, 749 (2001).
[15] B. Bureau, X. H. Zhang, F. Smektala, J. Adam, J. Troles, H. Ma, C. Boussard-Plèdel, J. Lucas, P. Lucas, D. L. Coq, M. R. Riley, and J. H. Simmons, J. Non-Cryst. Solids **345-346**, 276 (2004).
[16] P. Jóvári, I. Kaban, J. Steiner, B. Beuneu, A. Schöps, and M. A. Webb, Phys. Rev. B **77**, 035202 (2008).
[17] J.-H. Eom, Y.-G. Yoon, C. Park, H. Lee, J. Im, D.-S. Suh, J.-S. Noh, Y. Khang, and J. Ihm, Phys. Rev. B **73**, 214202 (2006).
[18] K. R. Symon, *Mechanics*, 3rd ed. (Addison-Wesley, Reading, MA, 1979).
[19] J. Ihm, A. Zunger, and M. L. Cohen, J. Phys. C **12**, 4409 (1979).
[20] G. B. Bachelet, D. R. Hamann, and M. Schluter, Phys. Rev. B **26**, 4199 (1982).
[21] X. Gonze, R. Stumpf, and M. Scheffler, Phys. Rev. B **44**, 8503 (1991).
[22] H. J. Monkhorst and J. D. Pack, Phys. Rev. B **13**, 5188 (1976).
[23] V. Weidenhof, I. Friedrich, S. Ziegler, and M. Wuttig, J. Appl. Phys. **86**, 5879 (1999).
[24] D. Wamwangi, W. Njoroge, and M. Wuttig, Thin Solid Films **408**, 310 (2002).